

## An approach towards understanding the structure of complex molecular systems: the case of lower aliphatic alcohols

To cite this article: Aleksander Vrhovšek *et al* 2010 *J. Phys.: Condens. Matter* **22** 404214

View the [article online](#) for updates and enhancements.

### You may also like

- [Local structure and dynamics of tungsten oxide-based glasses: insights from concurrent neutron diffraction and Compton scattering](#)

Matthew Krzystyniak, Kacper Drubicki, Istvan Tolnai *et al.*

- [Comparison of interatomic potentials of water via structure factors reconstructed from simulated partial radial distribution functions: a reverse Monte Carlo based approach](#)

Zsuzsanna Steinczinger, Pál Jóvári and László Pusztai

- [Short-range structure of barium tellurite glasses and its correlation with stress-optic response](#)

Amarjot Kaur, Atul Khanna and Margit Fábíán

# An approach towards understanding the structure of complex molecular systems: the case of lower aliphatic alcohols

Aleksander Vrhovšek<sup>1,2</sup>, Orsolya Gereben<sup>1</sup>, Szilvia Pothoczki<sup>1</sup>,  
Matija Tomšič<sup>2</sup>, Andrej Jamnik<sup>2</sup>, Shinji Kohara<sup>3</sup> and  
László Pusztai<sup>1</sup>

<sup>1</sup> Research Institute for Solid State Physics and Optics, Hungarian Academy of Sciences,  
H-1525 Budapest, PO Box 49, Hungary

<sup>2</sup> Faculty of Chemistry and Chemical Technology, University of Ljubljana, Aškerčeva 5,  
SI-1001 Ljubljana, Slovenia

<sup>3</sup> Research and Utilization Division, Japan Synchrotron Radiation Research Institute (JASRI,  
SPring-8), 1-1-1 Koto, Sayo-cho, Sayo-gun, Hyogo 679-5198, Japan

E-mail: [aleksander.vrhovsek@gmail.com](mailto:aleksander.vrhovsek@gmail.com)

Received 18 February 2010, in final form 16 April 2010

Published 22 September 2010

Online at [stacks.iop.org/JPhysCM/22/404214](http://stacks.iop.org/JPhysCM/22/404214)

## Abstract

An extensive study of liquid aliphatic alcohols methanol, ethanol, and propanol, applying reverse Monte Carlo modelling as a method of interpretation of diffraction data, is presented. The emphasis is on the evaluation of several computational strategies in view of their suitability to obtain high quality molecular models via the reverse Monte Carlo procedure. A consistent set of distances of closest approach and fixed neighbour constraints applicable to all three investigated systems was developed. An all-atom description is compared with a united-atom approach. The potentialities of employment of neutron diffraction data of completely deuterated and isotopically substituted samples, x-ray diffraction data, and results of either molecular dynamics or Monte Carlo calculations were investigated. Results show that parallel application of x-ray and neutron diffraction data, the latter being from completely deuterated samples, within an all-atom reverse Monte Carlo procedure is the most successful strategy towards attaining reliable, detailed, and well-structured molecular models, especially if the models are subsequently refined with the results of molecular dynamics simulations.

(Some figures in this article are in colour only in the electronic version)

## 1. Introduction

Many of the most important materials that surround us in everyday life happen to be molecular liquids. Interestingly, the level of understanding the structure and properties of these systems almost never matches their abundance and importance. Often their organization on a molecular level is governed by different association forces, resulting in a structure that is very complex. Such systems are classified as complex molecular liquids.

It is a well known fact that microscopic structure determines macroscopic properties. Hence it is of utmost importance to know the microscopic structure in as much

detail as possible to be able to better understand and predict macroscopic properties (thermodynamic data) from the most direct, structural point of view. Consequently, structural investigations of different molecular liquids have been an ongoing topic of research for many years. Diffraction techniques of various kinds (e.g. x-ray diffraction (XRD), neutron diffraction (ND), electron diffraction) are among the most powerful methods of assessing the structure of various materials. Having in mind the importance of the structure of molecular liquids, it is not surprising that these techniques have been extensively applied to such systems since the inception of particular methods (e.g. XRD has been used in the investigation of various molecular liquids for around a

century) [1–3]. Despite a significant improvement in the quality of measurement, data, and interpretation there are still many questions to be answered, especially when we move to more and more complex examples.

Lower aliphatic alcohols could be considered as fairly common, chemically relatively simple molecular liquids. And yet they all possess a polar hydroxylic group, which serves as a site for hydrogen bonding, and a nonpolar alkyl tail. Hydrogen bonds and the dual character of alcohols, in terms of their molecular polarity, are expected to bring about rather complex structure that changes with the length of the alkyl chain. Therefore, although relatively simple, aliphatic alcohols could be taken as the prototype of complex molecular liquids. Due to their availability, abundance, importance, and complex microscopic structure they have been widely investigated by various experimental methods and interpretation techniques for many years.

The earliest diffraction studies of alcohols employed XRD and relied solely on the well known Bragg law emanating from the crystal lattice concept [2, 3]. Obviously, such an approach could provide only vague, qualitative insight into the structure. Over the years analysis evolved to various, Fourier transform based techniques that have been used on XRD [4–12] and later, on ND [4–6, 13–18] data. All of these methods relied on the separation of the experimental total structure factor into intra- and inter-molecular contributions. The following Fourier inversion yielded the intra- and inter-molecular radial distribution functions. From them a few structural parameters could be deduced. A serious drawback of such an approach is that it is impossible to extract specific information about particle correlations without assumptions about the structure beyond the information that a diffraction experiment offers. Besides, the division to intra- and inter-molecular contributions necessarily introduces bias into the calculation. Employment of isotopic substitution to the ND samples (making use of partially deuterated alcohol molecules) [6, 13, 14] offered the possibility of only partial extraction of some particular particle distribution functions, depending on the isotopic composition of the samples measured.

With the advent of computer simulations, namely Monte Carlo (MC) and molecular dynamics (MD), these numerical methods have been utilized in the investigations of lower alcohols, mostly of methanol [13, 19–33]. The results are particle configurations that offer a possibility for calculating particle distribution functions. Unfortunately, diffraction data have not been used directly during the course of the simulations in any way—except sometimes for the final evaluation via the Fourier transform of the resulting distribution functions, yielding a structure factor of the model that could be compared to the experimental one [13, 19–24, 33]. Therefore the agreement of the produced models with the diffraction data heavily depends on the choice of the potential field for the simulation and could, in the most favourable cases, be termed only as semi-quantitative.

Everything mentioned so far calls for the employment of an approach that could take advantage of the virtues of the methods mentioned above while omitting most of their disadvantages and extracting as much structural information

from the experimental data as possible with the least of presumptions about the structure. Inverse methods of computer simulation offer such possibilities. To our best knowledge there has been only one empirical potential structure refinement [34] and one united-atom reverse Monte Carlo (RMC) study [35] on methanol reported up to now. Therefore we decided to perform an extensive study of liquid aliphatic alcohols applying RMC modelling [36] as a method of interpretation of diffraction data. The ultimate goal of the study is to devise a scheme applicable also to similar molecular systems that have not been studied by RMC so far. The choice of alcohols as a system was also driven by the fact that there is a great wealth of information from previous studies by other methods which could be used as a source for the comparison and evaluation of our approach. In this paper we report on simulation details and fits to the experimental data that could be achieved for the cases of methanol, ethanol, and propanol. We compare the performance of the protocol regarding the choice of input data and details of the molecular model (all-atom versus united-atom models).

## 2. Experimental and computational methods

### 2.1. Experiment

X-ray diffraction measurements were conducted at the SPring-8 synchrotron radiation facility in Japan, using the single-detector diffractometer setup of the BL04B2 high-energy x-ray diffraction beamline. The energy of x-ray photons was 61.7 keV, facilitating the easy access of a scattering vector range up to about  $16 \text{ \AA}^{-1}$ . Corrections to yield structure factors have been made by standard procedures such as for instance described in [37]. Alcohol samples of methanol, ethanol, and propanol were purchased from Fluka (Taufkirchen, Germany; purity > 99.5%) and were used without further treatment. Neutron diffraction data were acquired from the literature [14–16, 18].

### 2.2. Auxiliary molecular dynamics and Monte Carlo calculations

MD simulations for methanol, ethanol, and propanol were conducted within the canonic ensemble employing an OPLS all-atom force field [25, 26] with rigid bond lengths, and flexible bond and dihedral angles with dihedral constraints applied. The density, number of particles, and temperature were kept the same as in RMC calculations (see below). Partial radial distribution functions (PRDFs) were averaged over 26 configurations, gathered at 2 ps steps between 50 and 100 ps of the MD run. Furthermore, we have tested the representation with atomic groups through configurational biased MC calculations within the isothermal–isobaric ensemble employing the TraPPE united-atom force field [27]. Simulations of methanol were conducted by applying the Towhee package [38], while MC results for ethanol and propanol were taken from a work already published [22]. The number of particles and temperature were kept the same as in RMC calculations; pressure was set to 101.325 kPa. Random translational and rotational moves of the whole molecule, partial regrowth of the molecule, and

simulation box volume change were performed. Maximum displacements were adjusted during the simulation to achieve target acceptance rates (0.3 for translation and rotation, and 0.5 for volume change). Starting from the pre-equilibrated configuration, the simulation was run for an additional 20 000 MC cycles which were followed by a production run. Altogether 100 configurations were collected every 2000 MC cycles.

### 2.3. Reverse Monte Carlo modelling

Diffraction, MD, and MC data were modelled sequentially and simultaneously in the framework of the RMC technique, applying RMC++ code [39]. Prior to the construction of the initial configurations, a conformational search of the molecular structures had been performed using the programme MacroModel, part of the Schrödinger package [40]. The molecular model with the lowest energy was replicated onto the  $11^3$  equidistant grid points placed in a cubic cell. Replicas were randomly rotated and displaced for a small randomly chosen translational vector. Cell edge lengths that gave proper density at 25 °C were ascribed (see table 2). These configurations were input in the RMC procedure without any experimental restraints (i.e. XRD or ND data) apart from distances of closest approach and intra-molecular connectivity (fixed neighbour constraints (FNCs) [39, 41]), performing a kind of hard sphere simulation, up to a point where positions of atoms were random enough. Randomness was checked by tracking the distribution of displacements of representative atom types (atoms from the backbone of the molecule) from their original positions. Care was taken so that the width of the distribution was similar in all starting configurations.

In order to explore the method and its implementation to alcohols, it is necessary to write down the basic equations that relate microscopic structure in the RMC models to the experimental diffraction data. The usual way of structure description, while dealing with isotropic multicomponent systems is in terms of PRDFs. If the system consists of  $n$  components (e.g.  $n$  distinct types of atoms), there are

$$N_{\text{PRDF}} = \frac{n(n+1)}{2}. \quad (1)$$

PRDFs to be calculated to completely describe the particle pair-wise correlations (we shall denote PRDF between components  $i$  and  $j$  as  $g_{ij}$ ). However, this description is confined to real space while the experimental information is obtained in reciprocal space. Therefore, partial structure factors  $A_{ij}(Q)$ , derived from the Fourier transform of the PRDFs, are defined as

$$A_{ij}(Q) = 1 + \frac{4\pi\rho_0}{Q} \int_0^\infty [g_{ij}(r) - 1]r \sin(Qr) dr, \quad (2)$$

where  $\rho_0$  is the average atomic number density of the sample and  $Q$  is the scattering vector length. Individual contributions of the partial structure factors to the total scattering vary with the concentration of the constituents, expressed as amount fractions  $c_i$ , and their scattering response (scattering amplitude) that depends on the type of radiation and atomic

**Table 1.** Relative weights of OH correlations.

	Methanol	Ethanol	Propanol
ND	0.102	0.045	0.025
XRD	0.287	0.143	0.086

species considered—expressed as the coherent bound neutron scattering length  $\bar{b}_i$  for ND and the  $Q$ -dependent x-ray scattering factor  $f_i(Q)$  for XRD. The cumulative contribution of all partial correlations could then be calculated as the total scattering structure factor  $S(Q)$  that for ND reads

$$S_N(Q) = 1 + \sum_{i,j \geq i}^n (2 - \delta_{ij}) c_i c_j \bar{b}_i \bar{b}_j [A_{ij}(Q) - 1] * \left( \sum_{i=1}^n c_i \bar{b}_i \right)^{-2} \quad (3)$$

and for XRD

$$S_X(Q) = 1 + \sum_{i,j \geq i}^n (2 - \delta_{ij}) c_i c_j f_i(Q) f_j(Q) [A_{ij}(Q) - 1] * \left( \sum_{i=1}^n c_i f_i(Q) \right)^{-2}, \quad (4)$$

where  $\delta_{ij}$  is Kronecker delta. The second sum is included for normalization. Consequently, both total scattering structure factors (TSSF) tend to 1 at large  $Q$ . TSSF is the quantity that can be compared to the experimental diffraction data; scattering intensity, when all other contributions apart from the coherent interference term are removed and the same normalization is applied, corresponds to TSSF. Such treatment of the experimental data (called renormalization and background correction) can be achieved within the RMC++ algorithm as long as the contribution of these unwanted effects stays within reasonable limits. Most problematic in this respect is modelling of ND data of materials with high hydrogen ( $^1\text{H}$ ) content, like alcohols, especially when they are not completely deuterated, as they produce high incoherent inelastic scattering that can exceed the interference signal by several orders of magnitude.

It is instructive to check how the contributions of the most structurally significant correlations, namely O–O, O–H, and H–H, represented by respective partial structure factors, change with the length of the alkyl chain. These three correlations tell us the most about the hydrogen bond network. In table 1 we give the cumulative relative weights of the three OH correlations of methanol, ethanol, and propanol for ND and XRD (the latter data are given at  $2 \text{ \AA}^{-1}$ ). We can see that the OH contribution falls rapidly as the chain grows and that the numbers for XRD are consistently higher than for ND albeit both are rather low. This, of course, does not assign any superiority of XRD to ND but is merely the consequence of the almost complete insensitivity of XRD to hydrogen. In other words, XRD offers only information about carbon and oxygen correlations, whereas ND provides broader information about all atoms in the system including hydrogen to a great extent. We can rightfully expect a combination of the two methods to lead to the most conclusive results.

Another point worth mentioning is the very high number of PRDFs necessary to adequately describe configurations of

**Table 2.** Basic parameters of RMC simulations.

Type <sup>a</sup>	Cut-off <i>d</i> (Å)	FNC		Atomic number density	
		Type <sup>b</sup>	( <i>d</i> <sub>1</sub> – <i>d</i> <sub>2</sub> ) (Å)	Sample	$\rho_0$ (Å <sup>-3</sup> )
C–C	3.1	C–C	1.47–1.59	Methanol	0.089 2890
C–O	2.9	C–H	1.04–1.14	Ethanol	0.092 3807
C <sub>H3</sub> –O <sup>c</sup>	2.4	C–O	1.36–1.48	Propanol	0.096 6105
C–H	2.2	O–H	0.91–1.03		
C–H <sub>O</sub>	2.1	C–C–C	2.40–2.70		
C <sub>H3</sub> –H <sub>O</sub> <sup>d</sup>	2.2	C–C–H	2.03–2.29		
O–O	2.3	C–C–O	2.27–2.57		
O–H	2.0	C–O–H	1.79–2.09		
O–H <sub>O</sub>	1.4	O–C–H	1.92–2.18		
H–H	1.8	H–C–H	1.66–1.88		
H–H <sub>O</sub>	1.8				
H <sub>O</sub> –H <sub>O</sub>	1.5				

<sup>a</sup> C<sub>H3</sub>—methyl carbon, H<sub>O</sub>—hydroxylic hydrogen.

<sup>b</sup> FNC refers to terminal atoms in the notation.

<sup>c</sup> Relates only to propanol. <sup>d</sup> Relates to ethanol and propanol.

aliphatic alcohols, even for the lowest ones. For example, if we take methyl, methylene, and hydroxyl hydrogen atoms as three separate atom types, we have already 10 different PRDFs for methanol and this number leaps to 21 for ethanol. This means that we would need the same number of independent experimental data sets of indefinite *Q*-range and containing no errors to completely describe the system. This is clearly unattainable. Any significant error in the data brings about uncertainty in the calculation that increases considerably the number of distinct sets of PRDFs that fit to data equally well. Therefore, it is better to restrict the calculation only to experimental data sets of the lowest possible experimental error.

## 2.4. Computational strategies

The above two factors, the low weight of OH correlations and the lack of independent experimental data sets, leaves us with a highly indeterminate system to be solved. Hence, there is a need for additional strategies to limit the range of possible solutions. Such strategies may be grouped as follows.

**2.4.1. Making use of additional structural information about the system.** Excluded volume effects and chemical connectivity are two very basic properties that all molecular systems possess. In RMC++ we can make use of them via distances of closest approach (so-called ‘cut-offs’) and FNCs. While these restraints can efficiently prevent the system modelled from attaining physically improbable states, care has to be taken not to be over-restrictive when assigning the values; we have to let the system visit all significant points in the configuration space. The conformational search mentioned above proved to be very helpful in this respect.

**2.4.2. Employing additional experimental data.** Isotopic substitution enables us to obtain additional independent ND data sets, differing only in terms of the isotopic composition of the samples. While usual chemical and physical properties remain almost the same, neutron diffraction behaviour changes

markedly especially with hydrogen/deuterium substitution. Unfortunately, problems with incoherent inelastic scattering of hydrogen appear when samples are not completely deuterated. This directly contradicts the need for high quality data to offer a significant improvement to the RMC models.

**2.4.3. MD and MC computer simulations.** In contrast to RMC, these methods always employ certain interatomic potentials for generating model configurations. PRDFs stemming from these configurations can be used as additional restraints in RMC calculations [42, 43]. In this way, potentials may be included implicitly in the RMC procedure; moreover, this approach provides means for investigating the performance of different force-fields with respect to various structural characteristics of a system.

**2.4.4. Grouping of atomic species.** Atoms of the same kind that are very similar in view of their structural and chemical properties can be taken as one entity when calculating PRDFs, thus reducing the number of functions; note that this would be an actual ‘experimental situation’ in most cases. To whatever extent this approach eases the interpretation, it never reduces indeterminacy of the system at all. We have grouped together hydrogen as well as carbon atoms of methylene and methyl groups. Hence, we defined four different atom types for methanol (C, O, alkyl-H, and hydroxyl-H) and six for ethanol and propanol (methyl-C, methylene-C, O, methyl-H, methylene-H, hydroxyl-H). Note that, without this reduction, the number of atom types would increase to eight (or alternatively, the number of PRDFs to 36) in the case of propanol.

Another grouping approach has been often applied to model XRD data of alcohols and similar hydrogenous materials [7, 8, 22, 35, 44, 45]. As in this case (and never for ND!) only a very minute part of the scattering comes from hydrogen, H-atoms were not treated explicitly but rather as part of atomic groups. For aliphatic alcohols we shall, therefore, define methyl and methylene groups as fundamental scattering species in this approach. Hydroxylic hydrogen is to be treated separately, due to its structural importance.

We have thoroughly explored the potentialities of the above strategies for modelling the structure of complex molecular liquids, by applying them to the three systems we report about here.

## 3. Results and discussion

A uniform sequence of steps in RMC modelling had to be followed for all three liquid systems under investigation to be able to evaluate the potentialities and drawbacks of various computational strategies mentioned above. We have started with the choice of appropriate values of distances of closest approach (cut-offs) and FNCs. Intra-molecular distances from the conformational search and van der Waals radii of atoms were useful initial guesses for the reasonable starting values of FNCs and cut-offs, respectively. These initial sets of restraints were refined during the course of the following RMC calculations (modelling ND and XRD data) leading to the final

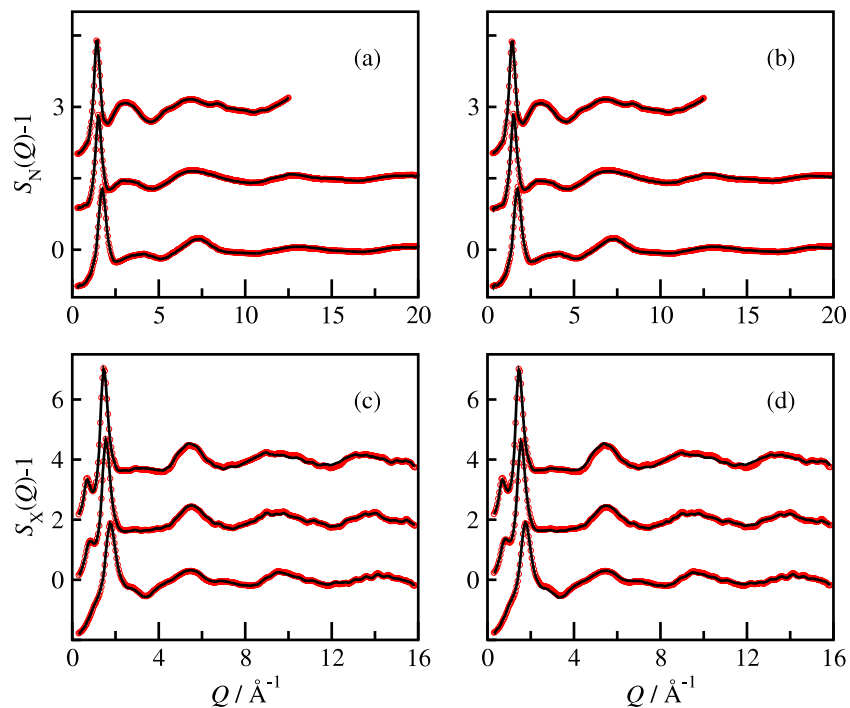


**Figure 1.** RMC fits (lines) to diffraction data (circles) for methanol (bottom curves), ethanol (middle curves), and propanol (top curves). (a) and (b)  $S_N(Q)$ , (c) and (d)  $S_X(Q)$ . (a) and (c) ND + XRD, (b) and (d) ND + XRD + MD.

values that we report in table 2. During the refinement, special care was taken on the peculiarities of the PRDFs (e.g. too sharp or sluggish edges, peak splitting) that can result from an unsuitable choice of either FNCs or cut-offs.

Thereafter, we have proceeded to the stepwise modelling of ND, XRD, and MD data. Overall, the simulation was performed in three steps. In each of them, one more data set was added (always starting from ND, then XRD, and lastly MD), creating a sequence of three RMC models for each alcohol, differing in the number of data sets applied ('ND', 'ND + XRD', 'ND + XRD + MD'). This way, contributions of individual data sets and of their combinations to the microscopic structure of the models could be explored. RMC fits to the experimental diffraction data for ND + XRD and ND + XRD + MD calculations are shown in figure 1. Respective graphs for the first, ND step, show no differences from the ones presented and are therefore omitted.

Close inspection of the plots reveals that all of the fits are very tight and do not show any significant discrepancies between each other. It is, however, much more instructive to see how the microscopic structure of the models, expressed in terms of PRDFs, evolves when additional data sets are involved in the simulation. While PRDFs, originating from correlations between the non-hydroxylic constituents and from their correlations with the  $-OH$  group do not show any marked change after the initial ND step of the simulation is completed, this does not apply to the three PRDFs that correspond to the hydroxyl group. Results for the three most interesting PRDFs from the hydroxylic group are given in figure 2. We can see that the RMC simulation with ND data, as the sole experimental restraint, does not result in any structural features apart from the strong intra-molecular O–H peak in the depicted

hydroxyl PRDFs. Taking into consideration the very low relative weights of OH correlations, given in table 1, this finding is hardly surprising. However, the situation changes when XRD data are input in the RMC procedure. While the O–H and H–H functions still do not change significantly, the O–O PRDF shows a well defined peak for all three systems under consideration. The distance where it appears corresponds very well with reported O–O distances between hydrogen bonded hydroxyl groups of alcohols [8, 9, 15, 16, 21, 23] and with the result of our MD simulations. The last step in the procedure, employment of the MD data, results in well defined structural features in all three hydroxyl PRDFs, extending much further from the main peak. It can be seen that very good agreement between RMC results and MD-based PRDFs was not reached at the expense of any significant deterioration of the RMC fit to either ND or XRD experimental data (see figure 1).

Another approach to increase the information content available from the experimental data is the already mentioned employment of isotopically substituted samples in ND. To test this strategy, we have performed simultaneous RMC modelling of the three ND data sets for isotopically substituted samples of methanol— $CD_3OD$  (sample A),  $CD_3OH/D$  (sample B, equimolar mixture of A and C), and  $CD_3OH$  (sample C)—that were published by Adya *et al* [14] ('3ND' calculation). Moreover, we have also modelled the three ND data sets together with our XRD data ('3ND + XRD' calculation). We have used the values of  $\bar{b}_i$  from [14] while the rest of the RMC parameters were kept the same as in all other calculations. Fits to diffraction data are presented in figure 3(a). It is obvious that the quality of the two fits for sample A does not differ significantly from that of the ND + XRD fit to ND data shown in figure 1(a). However, the quality of the fit

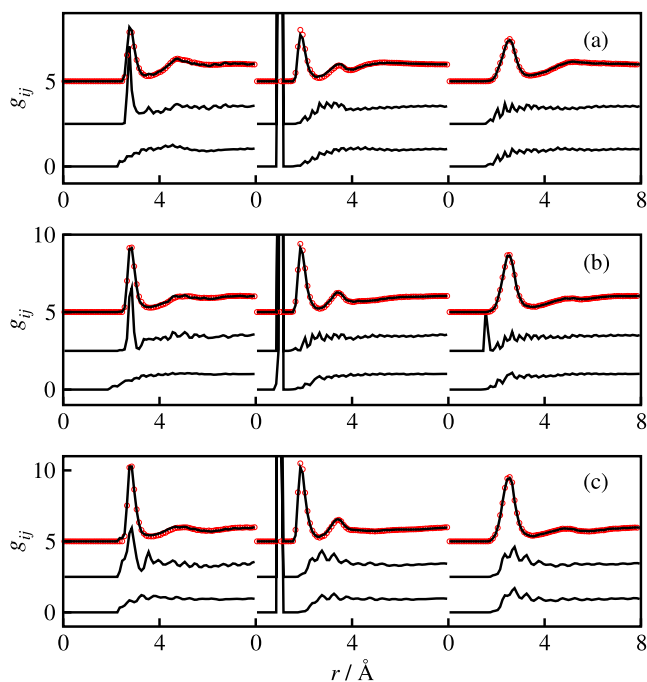


**Figure 2.** PRDFs of the hydroxylic group (left panels:  $g_{OO}(r)$ ; centre:  $g_{OH}(r)$ ; right:  $g_{HH}(r)$ ) for methanol (a), ethanol (b), and propanol (c). Lines represent RMC results (bottom: ND, middle: ND + XRD, top: ND + XRD + MD), while circles represent results of MD simulations.

gradually deteriorates with the increasing content of  $^1\text{H}$ , which is obvious from the respective curves for samples B and C. Comparison of the three calculations (3ND, 3ND + XRD, and ND + XRD) in terms of the results for the three hydroxyl group PRDFs is given in figure 3(b). To ease the comparison, results of the MD simulation were added as they should, at least approximately, correspond to the expected distribution of

interatomic distances that are under consideration. We can see that the 3ND procedure results in generally more structured hydroxylic PRDFs, including the two functions involving hydrogen. However, closer inspection reveals that the main inter-molecular peaks for the O–O and O–H correlations appear at distances that are approximately  $0.5 \text{ \AA}$  lower than the generally accepted values between these atoms in H-bonded alcohols (see e.g. [8, 9, 15, 16, 21, 23]), while for the ND + XRD approach the O–O peak appears to be in much better agreement. We can also notice an unexpected split of the first peak of the H–H PRDF. For the 3ND + XRD calculation the O–O peak moves to the position predicted by both ND + XRD and MD. In fact, the whole function very much resembles the ND + XRD result which supports our considerations concerning weights of correlations from the previous section. However, the shift of the, now less intense, O–H peak still persists, while the split of the H–H peak diminishes to some extent. Taking into account all of the above observations, we may conclude that in the case of methanol, introduction of the additional ND data sets did not offer much improvement, if any at all, over the usage of only the most reliable data from the completely deuterated sample. In both cases, addition of XRD data was necessary to reach consistent results that were in fact very similar regardless of the number of ND data sets applied. We could hardly expect the situation to change considerably for higher alcohols since the weight of the hydroxyl hydrogen and oxygen decreases rapidly as the number of carbon atoms increases.

At this point it is timely to investigate the usability of computer simulations for our systems with particular emphasis on the two commonly applied representations, namely the all-atom and united-atom approaches. We compare results of MD simulations employing the OPLS force field as an example for the all-atom description and results of MC simulations employing the TraPPE united-atom force field as the example of the united-atom approach. PRDFs resulting from both

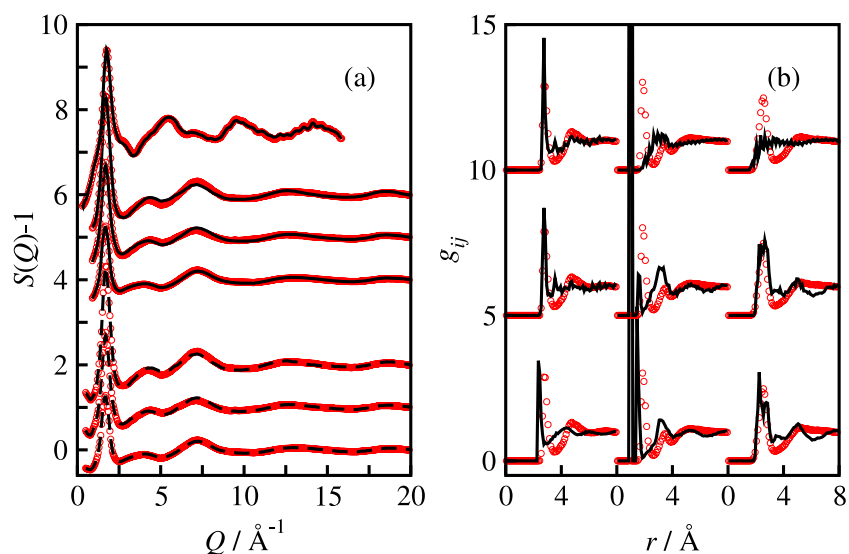


**Figure 3.** (a) RMC fits (dashed lines: 3ND, full lines: 3ND + XRD) to diffraction data (circles) for isotopically substituted methanol samples (both ‘curve-triplets’—bottom: sample A, middle: sample B, top: sample C). Uppermost curve: 3ND + XRD fit to XRD data. (b) PRDFs of the hydroxylic group (left panels:  $g_{OO}(r)$ ; centre:  $g_{OH}(r)$ ; right:  $g_{HH}(r)$ ) for 3ND (bottom row), 3ND + XRD (middle row), and ND + XRD (top row). Lines: RMC results, circles: MD simulation.

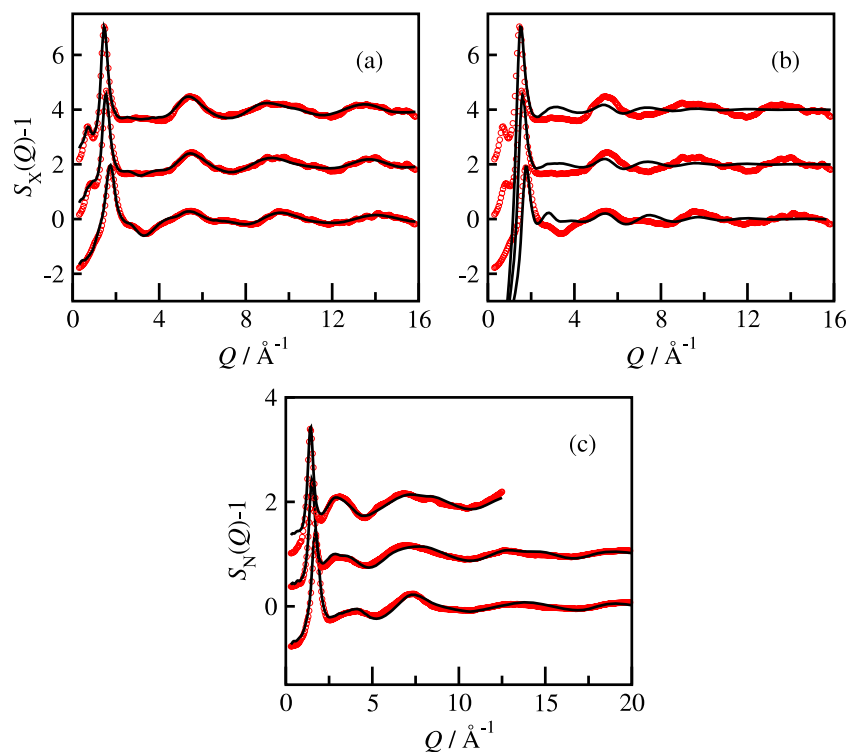


**Figure 4.** TSSFs from the computer simulations (lines) compared with the experimental diffraction data (circles) for methanol (bottom curves), ethanol (middle curves), and propanol (top curves). (a)  $S_X(Q)$  from MD (all-atom), (b)  $S_X(Q)$  from MC (united-atom), (c)  $S_N(Q)$  from MD (all-atom).

simulations were Fourier transformed to give the TSSFs that are compared with the experimental XRD and ND data as shown in figure 4. Concerning the united-atom representation it should be noted that it effectively prevents one from using ND data as hydrogen atoms (which are responsible for the most significant part of the ND signal) are not treated explicitly in this approach. Therefore, only XRD structure factors were calculated for the MC (united-atom) simulation. We can see that fits to the experimental values are much better for the all-atom description even though all of them are far from the tightness achieved via the RMC procedure (compare with figure 1). Most noteworthy is the almost complete misinterpretation of the high- $Q$  interval of XRD data by the united-atom approach, indicating the inability to accurately describe the very short range structure of our systems. However, when the PRDFs produced by (all-atom) MD simulations were input as the additional constraint in the RMC calculation, it was possible to achieve excellent agreement between RMC and MD PRDFs (see figure 2) while also retaining the consistency with experimental results (see figure 1). In other words, the models constructed by RMC (ND + XRD + MD) were in a much better agreement with diffraction data than MD models while the PRDFs did not show significant difference. Hence, it is reasonable to expect such kinds of improvement also for the united-atom approach. To test this expectation we have conducted two groups of united-atom calculations for all three liquids. The first group consisted of united-atom RMC simulations where XRD data were the only experimental restraint (XRD – UA).

In the second group, also PRDFs of the MC simulation were included as restraints (XRD + MC – UA). Agreement of both groups of calculations with the experimental XRD data is shown in figure 5. It is obvious that the agreement is good and comparable with the all-atom description for both groups of simulations. Only very minute deterioration from (a) towards (b) can be detected upon careful inspection. We should confirm that these findings go in line with results of similar calculations for the all-atom description (ND + XRD and ND + XRD + MD, see figure 1). Yet, the three hydroxyl PRDFs depicted in figure 6 are indicative of the shortcomings of this description. As we are limited only to XRD experimental data in the united-atom approach, PRDFs that result from simulations with only experimental diffraction restraints (figure 6(a)) do not show such a level of structural detail as the corresponding ones for the all-atom representation (see ND + XRD curves in figure 2). This fact is most obvious for  $g_{OO}$ , where in the present case we obtain a main peak that approximately matches the MC result in intensity and position only for methanol, while for the all-atom approach the agreement with MD results is good for all three liquids. For the XRD + MC – UA RMC simulation the agreement in terms of PRDFs is good, albeit the calculation is based only on one experimental data set and therefore is much more dependant on the results of MC simulation (that were previously shown not to be highly consistent with experimental data—see figure 4(b)). Overall, we should conclude that the united-atom approach is less reliable than the all-atom description.

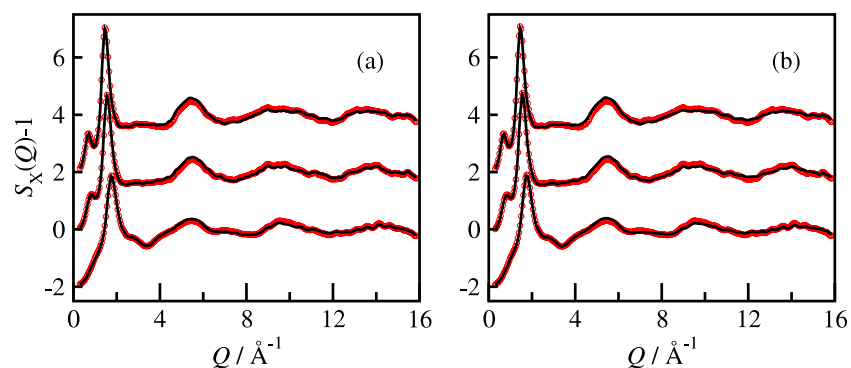


**Figure 5.** RMC fits (lines) to the experimental XRD data (circles) for the united-atom representation (bottom—methanol, middle—ethanol, top—propanol). (a) XRD – UA, (b) XRD + MC – UA.

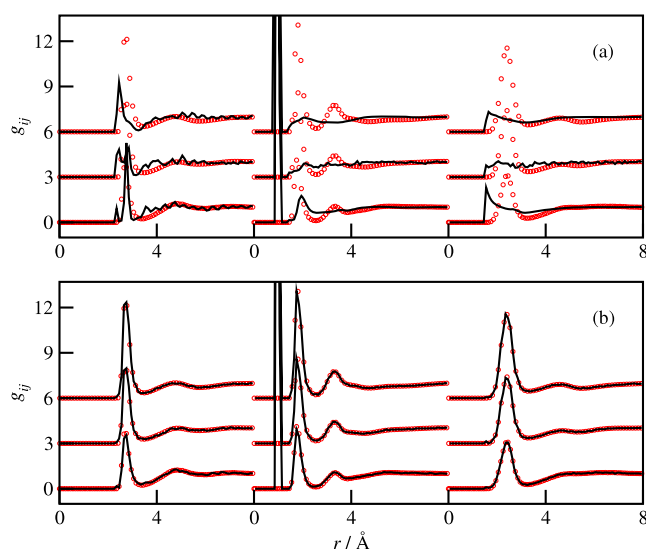


**Figure 6.** PRDFs of the hydroxylic group (left panels;  $g_{OO}$ ; centre:  $g_{OH}$ ; right:  $g_{HH}$ ) for methanol (bottom), ethanol (middle), and propanol (top). Lines ((a) XRD – UA, (b) XRD + MC – UA) represent RMC results, while circles represent results of MC simulation.

#### 4. Conclusion

We have extensively investigated the potentialities of several strategies to develop detailed structural models of the three lowest simple aliphatic alcohols within the framework of the RMC technique. Strategies were evaluated in terms of the agreement of the respective molecular models with diffraction data and structural features of the resulting partial radial distribution functions. We developed a consistent set of inter-molecular distances of closest approach (cut-offs) and intra-molecular FNCs. ND data alone were not enough to impose any significant structure to the hydroxylic PRDFs. We have shown for the case of methanol that introduction of the additional ND data sets from isotopically substituted samples did not offer much improvement, if any at all, over the usage of only the most reliable data from the completely deuterated sample. In both cases, addition of XRD data was necessary to reach consistent results that were in fact very similar regardless

of the number of ND data sets applied. Employment of PRDFs from the MD simulations in the RMC calculation lead to conclusive results for all PRDFs with structural features extending much further from the first inter-molecular peak. All RMC fits to diffraction data were found to be superior to the ones obtained for either MD OPLS all-atom or MC TraPPE united-atom models. However, when comparing the performance of the all-atom to united-atom models, in both RMC and direct MD or MC simulations, we may state that the united-atom approach is less suited to our problem than the all-atom description as it excludes the use of ND data and therefore reduces considerably the amount of available experimental restraints and is also inferior in the description of very short range interactions. Taking all of our findings into account, it should be stated that employment of both types of data, ND and XRD, within the all-atom RMC procedure together with carefully chosen cut-offs and FNCs and with subsequent refinement with MD-based PRDFs turned out to be the most successful strategy towards attaining reliable, detailed, and well-structured molecular models. This approach also shows the greatest potential for further work with higher aliphatic alcohols and similar molecular liquids.

#### Acknowledgments

We are grateful to Črtomir Podlipnik for performing the conformational search of the molecular structures. This work has been supported by a bilateral Slovenian–Hungarian travel grant No. SI-18/07.

#### References

- [1] Raman C V and Sogani C M 1927 *Nature* **119** 601
- [2] Stewart G W and Morrow R M 1927 *Phys. Rev.* **30** 232
- [3] Stewart G W and Skinner E W 1928 *Phys. Rev.* **31** 1
- [4] Sarkar S and Joarder R N 1993 *J. Chem. Phys.* **99** 2032–9
- [5] Sarkar S and Joarder R N 1994 *J. Chem. Phys.* **100** 5118–22
- [6] Weitkamp T, Neufeind J, Fischer H and Zeidler M 2000 *Mol. Phys.* **98** 125
- [7] Narten A H and Sandler S I 1979 *J. Chem. Phys.* **71** 2069–73
- [8] Narten A H and Habenschuss A 1984 *J. Chem. Phys.* **80** 3387–91
- [9] Magini M, Paschina G and Piccaluga G 1982 *J. Chem. Phys.* **77** 2051–6

- [10] Zachariassen W H 1935 *J. Chem. Phys.* **3** 158–61
- [11] Harvey G G 1938 *J. Chem. Phys.* **6** 111–4
- [12] Vahvaselkä K S, Serimaa R and Torkkeli M 1995 *J. Appl. Crystallogr.* **28** 189–95
- [13] Benmore C J and Loh Y L 2000 *J. Chem. Phys.* **112** 5877–83
- [14] Adya A K, Bianchi L and Wormald C J 2000 *J. Chem. Phys.* **112** 4231–41
- [15] Montague D G, Gibson I P and Dore J C 1981 *Mol. Phys.* **44** 1355
- [16] Montague D G, Gibson I P and Dore J C 1982 *Mol. Phys.* **47** 1405
- [17] Tanaka Y, Ohtomo N and Arakawa K 1984 *Bull. Chem. Soc. Japan* **57** 2569–73
- [18] Sahoo A, Sarkar S, Krishna P, Bhagat V and Joarder R 2008 *Pramana* **71** 133–41
- [19] MacCallum J L and Tieleman D P 2002 *J. Am. Chem. Soc.* **124** 15085–93
- [20] Kosztolanyi T, Bako I and Palinkas G 2003 *J. Chem. Phys.* **118** 4546–55
- [21] Akiyama I, Ogawa M, Takase K, Takamuku T, Yamaguchi T and Ohtori N 2004 *J. Solut. Chem.* **33** 797–809
- [22] Tomšič M, Jamnik A, Fritz-Popovski G, Glatter O and Vlček L 2007 *J. Phys. Chem. B* **111** 1738–51
- [23] Thomas J L, Tobias D J and MacKerell A D 2007 *J. Phys. Chem. B* **111** 12941–4
- [24] Tomšič M, Fritz-Popovski G, Vlček L and Jamnik A 2007 *Acta Chim. Slov.* **54** 484–91
- [25] Jorgensen W L 1986 *J. Phys. Chem.* **90** 1276–84
- [26] Jorgensen W L, Maxwell D S and Tirado-Rives J 1996 *J. Am. Chem. Soc.* **118** 11225–36
- [27] Chen B, Potoff J J and Siepmann J I 2001 *J. Phys. Chem. B* **105** 3093–104
- [28] Svishchev I M and Kusalik P G 1994 *J. Chem. Phys.* **100** 5165–71
- [29] Gao J, Habibollahzadeh D and Shao L 1995 *J. Phys. Chem.* **99** 16460–7
- [30] Saiz L, Padro J A and Guardia E 1997 *J. Phys. Chem. B* **101** 78–86
- [31] Patel S and Brooks C L 2005 *J. Chem. Phys.* **123** 164502
- [32] Wang S and Cann N M 2007 *J. Chem. Phys.* **126** 214502
- [33] Tomšič M and Jamnik A 2008 Simple alcohols and their role in the structure and interactions of microemulsion systems *Microemulsions: Properties and Applications (Surfactant Science vol 144)* ed M Monzer (Boca Raton, FL: CRC Press) pp 143–83
- [34] Yamaguchi T, Hidaka K and Soper A K 1999 *Mol. Phys.* **96** 1159
- [35] Bakó I, Jedlovsky P and Pálincás G 2000 *J. Mol. Liq.* **87** 243–54
- [36] McGreevy R L and Pusztai L 1988 *Mol. Simul.* **1** 359
- [37] Kohara S, Suzuya K, Kashihara Y, Matsumoto N, Umesaki N and Sakai I 2001 *Nucl. Instrum. Methods Phys. Res. A* **467/468** 1030–3
- [38] <http://towhee.sourceforge.net>
- [39] Gereben O, Jovari P, Temleitner L and Pusztai L 2007 *J. Optoelectron. Adv. Mater.* **9** 3021–7
- [40] <http://www.schrodinger.com>
- [41] Evrard G and Pusztai L 2005 *J. Phys.: Condens. Matter* **17** S1–13
- [42] Pusztai L, Harsányi I, Dominguez H and Pizio O 2008 *Chem. Phys. Lett.* **457** 96–102
- [43] Pusztai L, Pizio O and Sokolowski S 2008 *J. Chem. Phys.* **129** 184103–6
- [44] Narten A H 1977 *J. Chem. Phys.* **67** 2102–8
- [45] Narten A H 1979 *J. Chem. Phys.* **70** 299–304